Partitioned densities of states in a resonant tunnelling structure

2000 J. Phys.: Condens. Matter 12 4053

(http://iopscience.iop.org/0953-8984/12/17/311)

J. Phys.: Condens. Matter **12** (2000) 4053–4066. Printed in the UK PII: S0953-8984(00)10842-2

Partitioned densities of states in a resonant tunnelling structure

Xuean Zhao

Zhejiang Institute of Modern Physics, Zhejiang University, Hangzhou, 310027, People's Republic of China

Received 5 January 2000, in final form 3 March 2000

Abstract. We analyse the properties of the partitioned densities of states in mesoscopic transport problems. In terms of an imaginary-potential model, a concise derivation of the local partial density of states (LPDOS) is given. Using a numerical method to calculate the functional derivative of the scattering matrix, a detailed study of different kinds of decomposed densities of states in double-barrier structures is carried out. We find that the dynamical local density of states $\mathrm{d}n_{\alpha\alpha}(x)/\mathrm{d}E$ and the global partial density of states (GPDOS) $\mathrm{d}N_{\alpha\alpha}/\mathrm{d}E$ in the nonclassical regime cannot be neglected in full quantum calculations.

1. Introduction

As is well known for mesoscopic conductors, electron dynamics is governed by quantum mechanics. Quantum effects resulting from interferences between the incident and reflected wavefunctions as well as from confinements play dominant roles in determining the transport properties of conductors. Among the quantities describing this quantum transport is the density of states (DOS), which is an important quantity in many fields such as those of thermodynamical systems, tunnelling spectroscopy, and scattering theory [1–3]. In the 1960s, Dashen, Ma, and Bernstein (DMB) [4] gave the DOS in terms of the scattering matrix. The system that they considered is a grand canonical ensemble and the volume of the system is infinite. The extracted dynamical density of states is dependent purely on the trace of the on-shell scattering matrix and its inverse matrix. The DMB relation is

$$\Delta\frac{\mathrm{d}N}{\mathrm{d}E} = \mathrm{Tr}\left(S^{\dagger}\frac{\mathrm{d}S}{\mathrm{d}E} - \frac{\mathrm{d}S^{\dagger}}{\mathrm{d}E}S\right)$$

where $\Delta\,\mathrm{d}N/\mathrm{d}E$ is the variation of the total DOS. With the advance of technology, real electronic devices have reached the size for which one must consider the size confinement effect and interference effects [5–7]. The electrical DOSs of a solid body are controlled by the possible interactions that the body can have with its environment [8]. In the 1990s, Büttiker and co-workers [9, 10] developed the concept of the DOS by decomposing the total DOS into partial densities of states (PDOSs) in the mesoscopic transport regime. The advantage of the partitioned DOS is that the dynamical quantum information can be obtained by using these PDOSs. For example, in recent low-frequency AC electronic transport studies [11–13, 15, 16] the PDOS is directly related to the displacement current. In particular, for the problem of multiple-probe scattering in mesoscopic conductors, each scattering matrix element can be directly related to the PDOS which describes the density of states for the possibility of

0953-8984/00/174053+14$30.00

transmission or reflection of that conductor. In addition to the role of the PDOS in the AC response, the local partial density of states (LPDOS) can be used to calculate the current-fluctuation spectrum at a single tunnelling tip [17]. Thus, many properties in transport problems for mesoscopic conductors can be predicted by the calculation of the PDOSs and the DOS.

In the semiclassical sense, there are four kinds of DOS which directly contribute to the electron transport in mesoscopic conductors [13, 14]. First, the global total DOS contributes the global transport density of states, and comes naturally from the external influence on the whole system when a reservoir increases its electrochemical potential slightly. Second, the global partial density of states (GPDOS) gives a partial total DOS for the transport density of states. The system response function, i.e., the admittance, is determined by the GPDOS. In the scattering theory, the form of the GPDOS is

$$\frac{\mathrm{d}N_{\alpha\beta}}{\mathrm{d}E} = \frac{1}{4\pi\mathrm{i}}\,\mathrm{Tr}\left(S^{\dagger}_{\alpha\beta}\frac{\mathrm{d}S_{\alpha\beta}}{\mathrm{d}E} - \frac{\mathrm{d}S^{\dagger}_{\alpha\beta}}{\mathrm{d}E}S_{\alpha\beta}\right) \tag{1}$$

where $S_{\alpha\beta}$ is the scattering matrix element which connects a probe of the conductor labelled by β to that labelled by α. The third PDOS is the injectivity, which describes the density of states injected from probe α regardless of which probe it finally exits from. The fourth PDOS is the reverse of the process of injectivity. It is the emissivity, which describes the particles incident from all probes and exiting only from the probe β. The above four densities of states are global properties of the density of states. Correspondingly, there are four local densities of states which describe the local partitioned properties of the density of states and arise in the scattering theory due to the presence of a an internal potential perturbations. That is, the long-range Coulomb interaction of the charges gives rise to an internal response to the external perturbation, and this internal response determines the local electrical states and is naturally expressed in terms of the LPDOS. The scattering theory and linear response [13] model predict the LPDOS as

$$\frac{\mathrm{d}n_{\alpha\beta}(\boldsymbol{r})}{\mathrm{d}E} = -\frac{1}{4\pi\mathrm{i}}\,\mathrm{Tr}\left[S^{\dagger}_{\alpha\beta}\frac{\mathrm{d}S_{\alpha\beta}}{\mathrm{d}U(\boldsymbol{r})} - \frac{\mathrm{d}S^{\dagger}_{\alpha\beta}}{\mathrm{d}U(\boldsymbol{r})}S_{\alpha\beta}\right]. \tag{2}$$

Thus, if one knows the functional dependence of the scattering matrix on the scattering potential landscape $U(\boldsymbol{r})$, the LPDOS can be obtained. Although in the investigation of AC transport the LPDOS has been widely used [18–21], to our knowledge there has been no explicit and concise derivation of this quantity. In this work we first give a derivation of the LPDOS based on the physical model, and then we give an example of a numerical calculation for the double-barrier structure for different PDOSs and LPDOSs. Finally, we discuss the special characteristics of these quantities and give our conclusions.

In the four kinds of PDOS and LPDOS, the essential PDOS element is the LPDOS. All of the other PDOSs can be constructed from the LPDOS. For instance, the local injectivity $\mathrm{d}\overline{n}_{\alpha}(r)/\mathrm{d}E$ and emissivity $\mathrm{d}\underline{n}_{\beta}(r)/\mathrm{d}E$ can be expressed by

$$\frac{\mathrm{d}\overline{n}_{\alpha}(\boldsymbol{r})}{\mathrm{d}E} = \sum_{\beta}\frac{\mathrm{d}n_{\alpha\beta}(\boldsymbol{r})}{\mathrm{d}E} \qquad \text{and} \qquad \frac{\mathrm{d}\underline{n}_{\beta}(\boldsymbol{r})}{\mathrm{d}E} = \sum_{\alpha}\frac{\mathrm{d}n_{\alpha\beta}(\boldsymbol{r})}{\mathrm{d}E}. \tag{3}$$

The global injectivity and the DOS are just integrals of the LPDOS [13, 14]:

$$\frac{\mathrm{d}N_{\alpha\beta}}{\mathrm{d}E} = \int \mathrm{d}\boldsymbol{r}\,\frac{\mathrm{d}n_{\alpha\beta}(\boldsymbol{r})}{\mathrm{d}E} \qquad \text{and} \qquad \frac{\mathrm{d}N}{\mathrm{d}E} = \sum_{\alpha}\frac{\mathrm{d}N_{\alpha}}{\mathrm{d}E}. \tag{4}$$

2. The local partial density of states

Consider a quasi-one-dimensional system. The unperturbed Hamiltonian is H_0. There are many probes denoted by α, β, γ, etc contacting with external reservoirs. We put an imaginary potential $-(\mathrm{i}\hbar\Gamma/2)\delta(x - x')$ at the position x'. The coefficient $-\mathrm{i}\hbar/2$ is introduced for convenience. Then the perturbed total Hamiltonian becomes

$$H = H_0 - \frac{\mathrm{i}\hbar\Gamma}{2}\delta(x - x'). \tag{5}$$

Here

$$H_0 = -\frac{\hbar^2}{2m}\,\partial_x^2 + U(x).$$

The perturbed Hamiltonian leads to $\delta U(x) = -(\mathrm{i}\hbar\Gamma/2)\delta(x - x')$. According to Schrödinger's equation, the particle flux continuity equation is then

$$\partial \int_\Omega |\psi(x,t)|^2\,\mathrm{d}x \Big/ \partial t + \oint_{\partial\Omega} J\,\mathrm{d}S = -\Gamma|\psi(x',t)|^2 \tag{6}$$

where Ω involves the point x' and $\partial\Omega$ is Ω's boundary surface, or

$$\partial_t|\psi(x,t)|^2 + \partial_x J = -\Gamma|\psi(x,t)|^2\delta(x - x'). \tag{7}$$

Since the Hamiltonian is independent of time, the wavefunction $\psi(x,t)$ is the steady-state scattering solution of the time-independent Schrödinger equation. In the latter we drop the time variable for convenience. The energy dependence of $\psi(x)$ is not explicitly written out due to on-shell scattering. Equation (6) and equation (7) indicate that the quantum mechanical probability current has a sink or a source at x', respectively, depending on the sign of Γ. Here J is the usual quantum mechanical current density. The variation of the current density is

$$\mathrm{d}J = -\Gamma|\psi(x')|^2. \tag{8}$$

The dwell time can be expressed by the relation [22, 24]

$$\mathrm{d}\tau_D = \frac{|\psi(x')|^2\,\mathrm{d}x'}{J} \tag{9}$$

where $\mathrm{d}\tau_D$ is the lifetime of a particle staying in the interval $[x', x' + \mathrm{d}x']$. Assume that the current J is the incident current; then the change of the current at the outgoing probes is expressed by equation (8). On substituting equation (8) into equation (9), the dwell time becomes

$$\mathrm{d}\tau_D = -\frac{\mathrm{d}J\,\mathrm{d}x'}{J\Gamma}. \tag{10}$$

In the scattering theory, one can express the variation of the probability flux in terms of the change in the transmission and reflection coefficients, δT and δR, i.e.

$$\mathrm{d}J = J(\delta R + \delta T). \tag{11}$$

In addition, the transmission and reflection are closely connected to the scattering matrix elements:

$$R = \mathrm{Tr}\left[s^\dagger_{\alpha\alpha}s_{\alpha\alpha}\right] \qquad \text{and} \qquad T = \mathrm{Tr}\left[s^\dagger_{\alpha\beta}s_{\alpha\beta}\right] \tag{12}$$

where the Greek letters denote the probes (contacts). We consider here the mean-field approximation. So the interactions between the particles and the perturbations are involved in the internal potential $U(x)$. Since the scattering matrix $s_{\alpha\beta}$ is not only a function of the

incident energy E but also a functional of the effective potential, we write $s_{\alpha\beta} = s_{\alpha\beta}(E, U(x))$. Expanding the scattering matrix to first order in the effective potential $U(x)$, one obtains

$$s_{\alpha\beta}(E, U + \delta U) = s^0_{\alpha\beta} + \int \frac{\delta s_{\alpha\beta}}{\delta U(x)}\, \delta U(x)\, \mathrm{d}x \tag{13a}$$

or

$$\delta s_{\alpha\beta}(E, U) = \int \frac{\delta s_{\alpha\beta}}{\delta U(x)}\, \delta U(x)\, \mathrm{d}x \tag{13b}$$

where the $s^0_{\alpha\alpha}$ are unperturbed scattering matrix elements. The variations of the reflection and transmission probabilities can be expressed by

$$\delta R = \mathrm{Tr}(s^\dagger_{\alpha\alpha}\, \delta s_{\alpha\alpha} + \delta s^\dagger_{\alpha\alpha}\, s_{\alpha\alpha}) = -\frac{\mathrm{i}\hbar\Gamma}{2}\, \mathrm{Tr}\left(s^\dagger_{\alpha\alpha} \frac{\delta s_{\alpha\alpha}}{\delta U(x')} - \frac{\delta s^\dagger_{\alpha\alpha}}{\delta U(x')} s_{\alpha\alpha} \right) \tag{14}$$

and

$$\delta T = \mathrm{Tr}(s^\dagger_{\alpha\beta}\, \delta s_{\alpha\beta} + \delta s^\dagger_{\alpha\beta}\, s_{\alpha\beta}) = -\frac{\mathrm{i}\hbar\Gamma}{2}\, \mathrm{Tr}\left(s^\dagger_{\alpha\beta} \frac{\delta s_{\alpha\beta}}{\delta U(x')} - \frac{\delta s^\dagger_{\alpha\beta}}{\delta U(x')} s_{\alpha\beta} \right). \tag{15}$$

In terms of equation (10) and equation (11) we obtain

$$\mathrm{d}\tau_D = \frac{\mathrm{i}\hbar}{2}\, \mathrm{Tr}\left[\left(s^\dagger_{\alpha\alpha} \frac{\delta s_{\alpha\alpha}}{\delta U(x')} - \frac{\delta s^\dagger_{\alpha\alpha}}{\delta U(x')} s_{\alpha\alpha} \right) + \left(s^\dagger_{\alpha\beta} \frac{\delta s_{\alpha\beta}}{\delta U(x')} - \frac{\delta s^\dagger_{\alpha\beta}}{\delta U(x')} s_{\alpha\beta} \right) \right]. \tag{16}$$

We can write for brevity

$$\mathrm{d}\tau_D = \frac{\mathrm{i}\hbar}{2} \sum_\beta \mathrm{Tr}\left(s^\dagger_{\alpha\beta} \frac{\delta s_{\alpha\beta}}{\delta U(x')} - \frac{\delta s^\dagger_{\alpha\beta}}{\delta U(x')} s_{\alpha\beta} \right) \mathrm{d}x'. \tag{17}$$

The well-known expression for the local density of states (LDOS) [25] is

$$\rho(x, E) = \sum_{n=1}^{N} \int \langle x|\phi_n(E')\rangle\langle\phi_n(E')|x\rangle \delta(E - E')\, \mathrm{d}E' = \sum_{n=1}^{N} \langle x|\phi_n(E)\rangle\langle\phi_n(E)|x\rangle. \tag{18}$$

Iannaccone [26] showed that the dwell time in the region Ω is directly related to the integral of the density of states $\rho(x, E)$ in that region. That is,

$$\rho_\Omega(E) = \sum_{n=1}^{N} \int_\Omega \langle x|\phi_n(E)\rangle\langle\phi_n(E)|x\rangle\, \mathrm{d}x = \sum_{n=1}^{N} \langle\phi_n(E)|\hat{P}_\Omega|\phi_n(E)\rangle = \frac{1}{2\pi\hbar} \sum_{n=1}^{N} \tau_D^{(n)}. \tag{19}$$

The expressions for the components of the dwell time read as

$$\mathrm{d}\tau^\alpha_D = 2\pi\hbar\rho^\alpha_\Omega. \tag{20}$$

Here we consider only one channel, and take $\Omega \to 0$. The states in the interval $[x', x' + \mathrm{d}x']$ are

$$\rho^\alpha(x')\, \mathrm{d}x' = \rho^\alpha_\Omega. \tag{21}$$

Then we have

$$2\pi\hbar\rho^\alpha(x')\, \mathrm{d}x' = \frac{\mathrm{i}\hbar}{2} \sum_\beta \mathrm{Tr}\left(s^\dagger_{\alpha\beta} \frac{\delta s_{\alpha\beta}}{\delta U(x')} - \frac{\delta s^\dagger_{\alpha\beta}}{\delta U(x')} s_{\alpha\beta} \right) \mathrm{d}x'. \tag{22}$$

Assuming that the current is incident from the probe α, and denoting the density of states by $\rho^\alpha(x) = \mathrm{d}n_\alpha(x)/\mathrm{d}E$, we finally obtain

$$\frac{\mathrm{d}n_\alpha(x')}{\mathrm{d}E} = \sum_\beta \left[-\frac{1}{4\pi\mathrm{i}}\, \mathrm{Tr}\left(s^\dagger_{\alpha\beta} \frac{\delta s_{\alpha\beta}}{\delta U(x')} - \frac{\delta s^\dagger_{\alpha\beta}}{\delta U(x')} s_{\alpha\beta} \right) \right] \tag{23}$$

where the index β runs all probes. The quantity in the square brackets is defined as the LPDOS [14]:

$$\frac{\mathrm{d}n_{\alpha\beta}(x)}{\mathrm{d}E} \equiv -\frac{1}{4\pi\mathrm{i}}\,\mathrm{Tr}\left(s^{\dagger}_{\alpha\beta}\frac{\delta s_{\alpha\beta}}{\delta U(x)} - \frac{\delta s^{\dagger}_{\alpha\beta}}{\delta U(x)}s_{\alpha\beta}\right). \tag{24}$$

In the last expression we drop the prime for the arbitrary position. In the semiclassical sense this expression shows the relation between the local partitioned density of states and the scattering matrix. We know that the scattering matrix contains only the dynamical information for the system. Thus, the LHS of equation (24) is the dynamical partial density of states which characterizes the density response in a local space to the external perturbations on the small-size conductor system. The advantage of this kind of partitioning is that it not only gives the density of states but also gives the directions of the particle's motion.

The decomposition of DOS is necessary for multiprobe conductors since not all of the DOSs contribute to a particular transport direction. A natural question arises: what fraction of the total DOS contributes to the transmission by particles incident on the probe (β) with unit current amplitude to the probe (α)? By using the LPDOS, we can answer this question clearly. From the above derivation we see that the point x has several properties. These properties can be represented by several states. The state $|\alpha, x, \beta\rangle$ contains the information that a particle incident on the probe α reaches the point x and then leaves that point and finally goes to the probe β. If we exchange the probe indices α and β, the meaning is different. The state $|\beta, x, \alpha\rangle$ represents a particle coming in from the probe β which is scattered from the point x and then goes to the probe α. In the next section we will support this argument with a numerical calculation.

In addition to the states $|\alpha, x, \beta\rangle$ and $|\beta, x, \alpha\rangle$, there are states $|\alpha, x, \alpha\rangle$ and $|\beta, x, \beta\rangle$. These states represent a particle that is incident from the probe α or β, reaches the point x, and then from there is reflected to the original probe. How many of these kinds of state there are in the energy interval $(E, E + \Delta E)$ can be calculated from the quantities $\mathrm{d}n_{\alpha\alpha}(x)/\mathrm{d}E$ and $\mathrm{d}n_{\beta\beta}(x)/\mathrm{d}E$. Here the position x can be in the nonclassical region and the quantities $\mathrm{d}n_{\alpha\alpha}(x)/\mathrm{d}E$ and $\mathrm{d}n_{\beta\beta}(x)/\mathrm{d}E$ are not zero. This property is unlike the semiclassical and classical results. Reference [14] gives a semiclassical example of these quantities based on phase-space arguments. In a one-dimensional single-barrier case it was shown that $\mathrm{d}n^{\mathrm{qc}}_{12}(x)/\mathrm{d}E = \mathrm{d}n^{\mathrm{qc}}_{21}(x)/\mathrm{d}E = (T/2)\,\mathrm{d}n(x)/\mathrm{d}E$ and $\mathrm{d}n^{\mathrm{qc}}_{11}(x)/\mathrm{d}E = R\,\mathrm{d}n(x)/\mathrm{d}E$ and also $\mathrm{d}n^{\mathrm{qc}}_{22}(x)/\mathrm{d}E = 0$ when particles are incident from probe 1, and x is located between probe 1 and the barrier. We will see from the numerical calculations that $\mathrm{d}n_{11}(x)/\mathrm{d}E$ is not accurately equal to the fraction R of the total density of states and $\mathrm{d}n_{22}(x)/\mathrm{d}E$ is not equal to zero. Here the superscript 'qc' represents the quasi-classical approximation. The results are the same for particles incident from probe 2 by exchanging the subscripts. The above expressions have a clear physical meaning. The expression $\mathrm{d}n^{\mathrm{qc}}_{12}(x)/\mathrm{d}E + \mathrm{d}n^{\mathrm{qc}}_{21}(x)/\mathrm{d}E = T\,\mathrm{d}n(x)/\mathrm{d}E$ states that the density of states for particles traversing from probe 1 to probe 2 plus from 2 to 1 is just a fraction of the transmission part of the total density of states. The sum of the reflection density of states is the reflected part of the total density of states.

In section 3 we will give a numerical example corresponding to the above discussion. At the outset, we would like to clarify that the purpose of this numerical study is to illustrate the importance of the partitioned density of states and not to model a typical resonant tunnelling device, whose structure is considerably more complicated [27]. In order to simplify the task of calculation, we use the rectangular-potential approximation and assume flat bands outside the barriers. We use atomic units in all of the numerical calculations, i.e., $\hbar = 1$, $e = 1$, and $2m = 1$.

3. Example

3.1. Numerical method

As mentioned in the previous section, the basic quantity is

$$\frac{\mathrm{d}n_{\alpha\beta}}{\mathrm{d}E} = -\frac{1}{4\pi\mathrm{i}}\left(s^{\dagger}_{\alpha\beta}\frac{\delta s_{\alpha\beta}}{\delta U(x)} - s_{\alpha\beta}\frac{\delta s^{\dagger}_{\alpha\beta}}{\delta U(x)}\right).$$

All of the other densities of states can be obtained as combinations of such quantities. The key task in calculating the LPDOS is to calculate the functional derivative and the scattering matrices. According to functional theory, a differential of a functional is the part of the difference $F[f+\delta f]-F[f]$ that depends on δf linearly. Here F is a functional. The variable is the function $f(x)$. The difference δf of the function may contribute to the functional $F[f+\delta f]$. So we can write

$$\delta F = \int \frac{\delta F[f(x)]}{\delta f(x)}\,\delta f(x)\,\mathrm{d}x \tag{25}$$

where the quantity

$$\frac{\delta F[f(x)]}{\delta f(x)} \tag{26}$$

is just the functional derivative of $F[f(x)]$ with respect to the function $f(x)$ at the point x [28]. Equation (26) is the rule for operating on $\delta f(x)$ to give the number $\delta F[f(x)]$. In the actual calculations the following method is applicable.

With the help of the rule, we expand $F[f+\delta f]-F[f]$ in terms of $\delta f(x)$. Keeping only the first-order term and taking care that the result is put into the form of the definition equation (26), one can explicitly express $\delta F[f(x)]/\delta f(x)$ by using the process

$$\lim_{\epsilon\to 0}\left[\frac{F[f(x)+\epsilon\phi(x)]-F[f(x)]}{\epsilon}\right] = \left\{\frac{\mathrm{d}(F[f(x)+\epsilon\phi(x)])}{\mathrm{d}\epsilon}\right\}_{\epsilon=0}$$
$$= \int \frac{\delta F[f(x)]}{\delta f(x)}\phi(x)\,\mathrm{d}x \tag{27}$$

where $\phi(x)$ is an arbitrary function. Taking $\phi(x)$ to be a delta function, $\delta(x-x')$, one obtains an explicit expression for the functional derivative:

$$\frac{\delta F[f(x')]}{\delta f(x')} = \left.\frac{\mathrm{d}(F[f(x)+\epsilon\phi(x)])}{\mathrm{d}\epsilon}\right|_{\epsilon=0}. \tag{28}$$

In our problem, the functional comprises the scattering elements $s_{\alpha\beta}(E, U(x))$. We first put a delta function with intensity ϵ at an arbitrary position in the structure. By calculating the scattering elements in the new potential and then letting the intensity ϵ approach zero, we obtain the quantity $\delta s_{\alpha\beta}/\delta U(x)$ and its conjugate $\delta s^{\dagger}_{\alpha\beta}/\delta U(x)$. For scattering matrix elements we use the transfer matrices and their combinations to get each scattering matrix element.

3.2. Results and discussion

Figure 2 shows the model of the resonant tunnelling diode and the simplified band structure. The particles are confined in the x-direction, while in the y-, z-directions the particles are free. Consider the two-channel case: one channel for particles moving with positive velocity v and the other channel for particles moving with negative velocity $-v$ at each probe α, β, γ, etc. We divide the system into three parts. The scattering is assumed to be elastic in

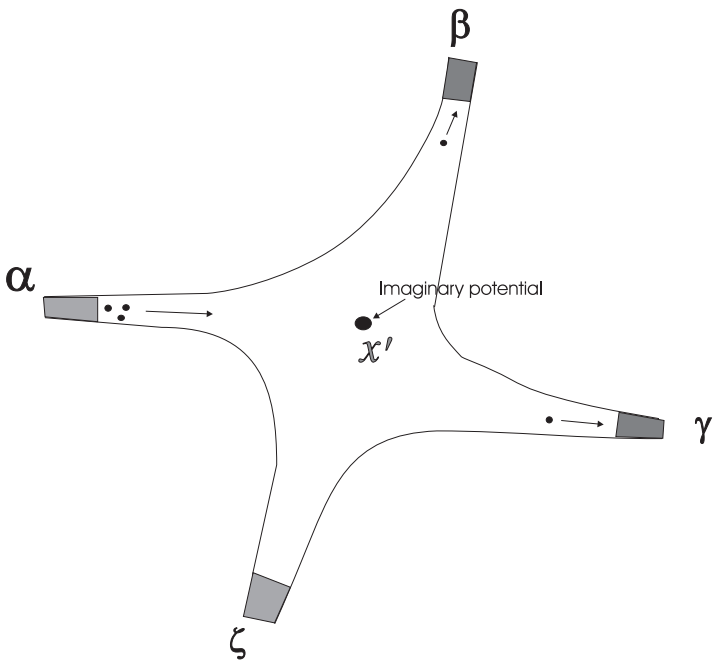

Figure 1. The model of the scattering structure. α, β, γ, and ζ represent the probes contacting with each of the reservoirs.

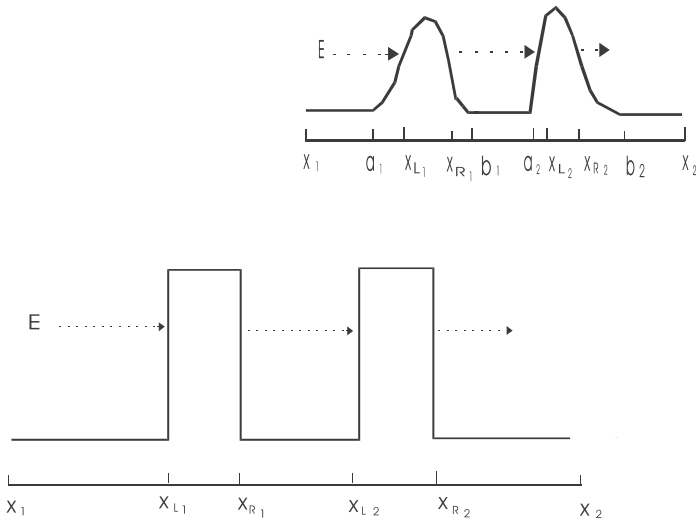

Figure 2. The band structure of the simplified double-barrier device. The inset is a real device potential profile. The boundaries of the system are located at x_1 and x_2. x_{L_1} and x_{R_1} are classical turning points for the left barrier; x_{L_2} and x_{R_2} are classical turning points for the right barrier. The scattering region is between a_1 and b_2.

the region $x_1 < x < x_2$. The potentials are located in the intervals $[a_1, b_1]$ and $[a_2, b_2]$, respectively. The classical turning points are denoted by x_{L_1} and x_{R_1} for the left barrier and x_{L_2} and x_{R_2} for the right barrier, respectively (see the inset). We denote the region $[x_1, x_{L_1}]$ as

$\Omega_{\rm I}$, $[x_{R_1}, x_{L_2}]$ as $\Omega_{\rm II}$, and $[x_{R_2}, x_2]$ as $\Omega_{\rm III}$, as shown in figure 2. The two barriers are equal, $V = V_1 = V_2 = 1.0$, and the potentials in regions $\Omega_{\rm I}$, $\Omega_{\rm II}$, and $\Omega_{\rm III}$ are equal to zero. We select parameters such that below the barrier there are two resonant peaks (see figure 3), in order to show the extent of the PDOS at different incident energies and around the resonant point. The incident energies are chosen to be at resonant transmission, near the resonant point, and at the middle transparent point—that is, $E_1 = 0.11$, $E_2 = 0.139$, $E_3 = 0.5896$, and $E_4 = 0.93$. We choose $x_1 - x_2 = 72\lambda_F$. Here λ_F is Fermi wavelength and is set equal to unity. The left barrier is located in the region $[0, \lambda_F]$ and the right barrier is in the region $[7\lambda_F, 8\lambda_F]$. In the following discussion, probe 1 is at x_1 and probe 2 is at x_2. The four incident energies are listed in the first column of table 1. The reflection probabilities and transmission probabilities are listed in columns 2 and 3, respectively.

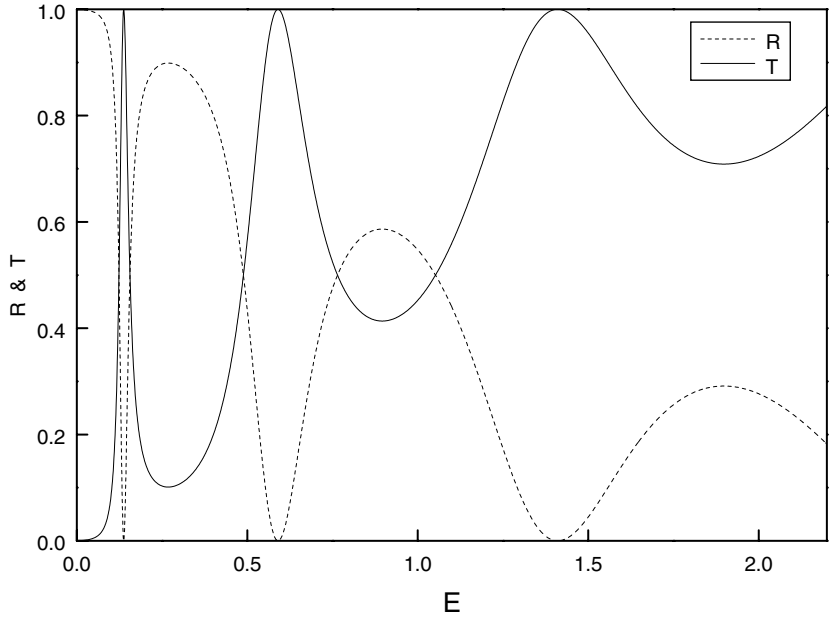

Figure 3. Transmission and reflection probabilities for the double-barrier structure shown in figure 2. The solid line represents the transmission probability and the dashed line represents the reflection probability.

Table 1. Energies, and reflection and transmission probabilities.

E	R	T
0.11	0.832	0.168
0.139	7.59×10^{-3}	0.9924
0.5896	2.03×10^{-5}	0.9999
0.93	0.582	0.418

Figures 4(a) and 4(b) show the distributions of the LPDOS quantities $\mathrm{d}n_{11}(x)/\mathrm{d}E$ in real space. In the region $\Omega_{\rm I}$, outside the two barriers, the quantities $\mathrm{d}n_{11}(x)/\mathrm{d}E$ oscillate due to the interference of the incident wave and the reflected wave. In figure 4(a) the dashed line is plotted at the resonant energy $E = E_3$. The reflection dynamical density of states $\mathrm{d}n_{11}(x)/\mathrm{d}E$ is zero. This is as expected, since in this case the particles are totally transmitted

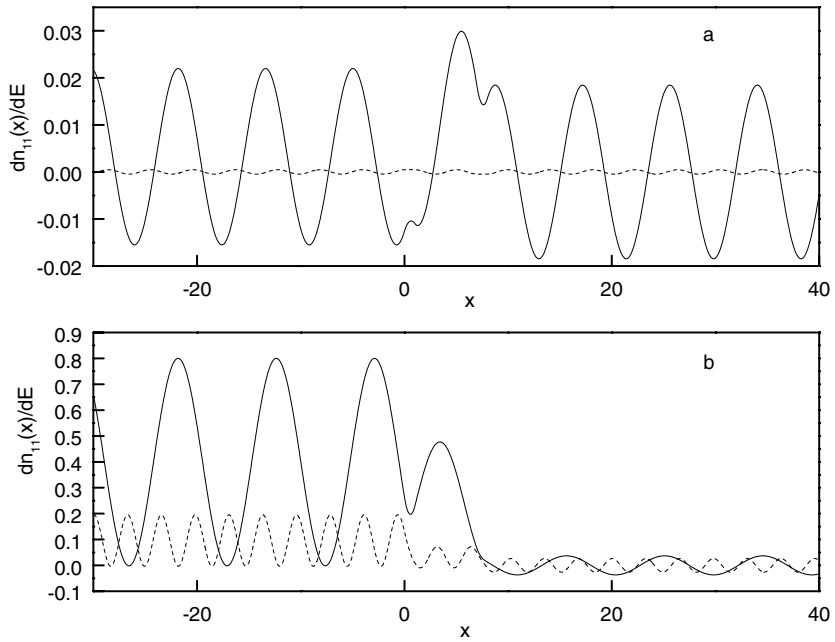

Figure 4. LPDOS $\mathrm{d}n_{11}(x)/\mathrm{d}E$ distributions in real space at different incident energies. (a) The solid line is at $E = E_2$ and the dashed line is at $E = E_3$ (resonant). (b) The solid line is at $E = E_1$ and the dashed line is at $E = E_4$.

to the outgoing probe 2. No states $|1, x, 1\rangle$ exist in the whole system. The reflections can occur only on the boundary of probe 2. But in this work we do not study boundary effects. We are only interested in the dynamical density of states in the transport processes. The solid line in figure 4(a) shows the LPDOS $\mathrm{d}n_{11}(x)/\mathrm{d}E$ with a slight reflection. It is not zero and it fluctuates. In the well, we find that $\mathrm{d}n_{11}(x)/\mathrm{d}E$ is not symmetric and is larger than that outside the well, despite the symmetry of the structure. This is because in the well the barrier located on the right reflects carriers back to probe 1 and contributes to $\mathrm{d}n_{11}(x)/\mathrm{d}E$, but the left barrier does not contribute to $\mathrm{d}n_{11}(x)/\mathrm{d}E$. This is unlike the case for the transmission density of states $\mathrm{d}n_{12}(x)/\mathrm{d}E$. Figure 5 shows the distribution of $\mathrm{d}n_{12}(x)/\mathrm{d}E$. It is different from the distribution of $\mathrm{d}n_{11}(x)/\mathrm{d}E$. Physically $\mathrm{d}n_{12}(x)/\mathrm{d}E$ represents the transmission states in the system. The distribution of $\mathrm{d}n_{12}(x)/\mathrm{d}E$ is always symmetric, as predicted by quasi-classical arguments. A typical characteristic is that at the resonant point the transmission density of states is almost located in the well. These results are confirmed by the explicit expression $\mathrm{d}n_{21}(x)/\mathrm{d}E = (T/2)\,\mathrm{d}n(x)/\mathrm{d}E$ given in reference [22], since at the resonant point the total density of states has a maximum peak in the well [23] as shown in figure 9, later. When the reflection probabilities increase, the LPDOS $\mathrm{d}n_{11}(x)/\mathrm{d}E$ becomes larger in the region Ω_{I} than those in the regions Ω_{II} and Ω_{III}. This is due to the particles having little opportunity to pass through the barriers. The global characteristics of $\mathrm{d}n_{11}(x)/\mathrm{d}E$ are shown in figures 6(a), 6(b). In this paper we do not consider the relaxation effect caused by reservoirs. The particles enter the scattering region only when they leave the probes; see figure 1. This is just like the case of a photon emitted from a black body. The relaxation of particles in the reservoirs can be dealt with using the relaxation time τ_ϕ [29, 30]. Thus, the GPDOSs are calculated by integration of the LPDOS over each region where the reservoir is not involved. Figure 6(a) shows that dramatic oscillations occur around the resonant energies in the region Ω_{III}. This has no classical

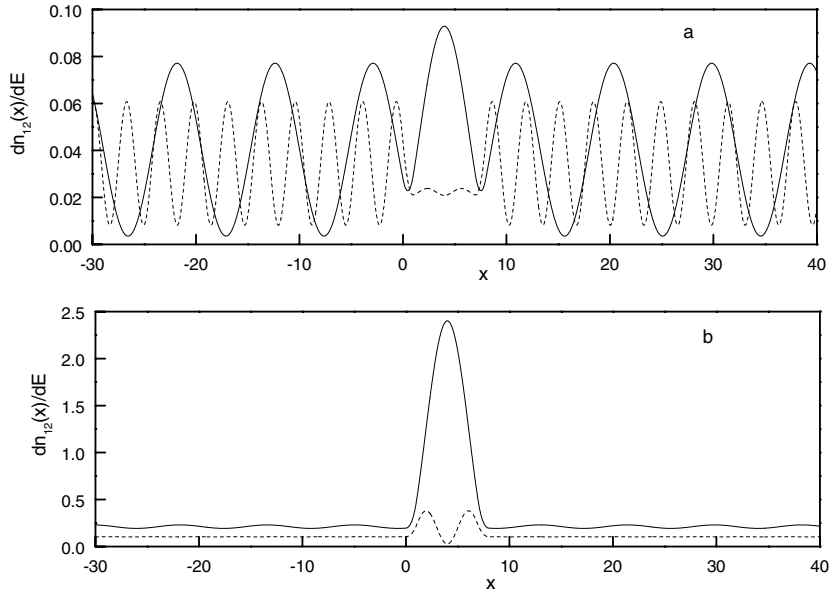

Figure 5. LPDOS $\mathrm{d}n_{21}(x)/\mathrm{d}E$ distributions in real space at different incident energies. (a) The solid line is at $E = E_1$ and the dashed line is at $E = E_4$. (b) The solid line is at $E = E_2$ and the dashed line is at $E = E_3$ (resonant).

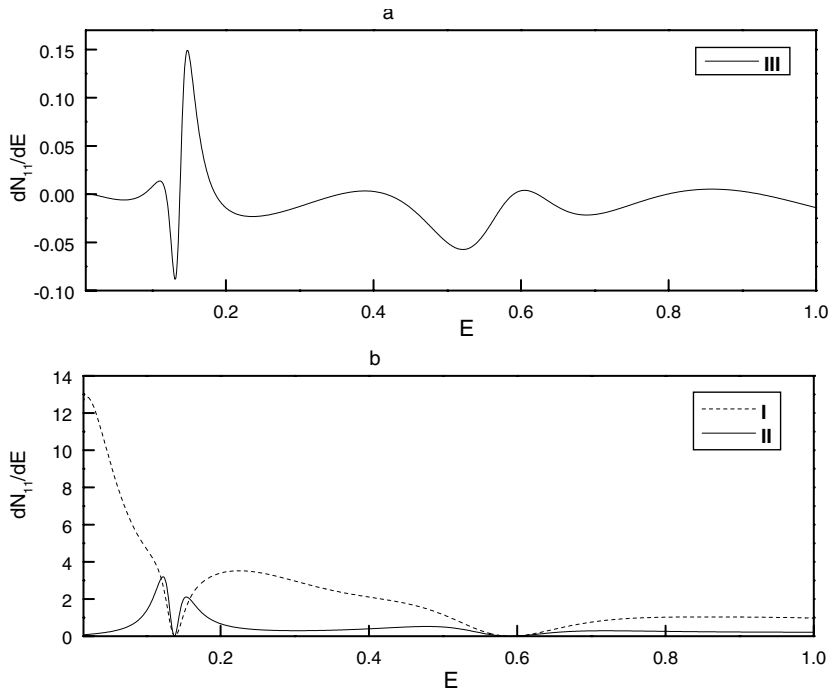

Figure 6. The global PDOS $\mathrm{d}N_{11}/\mathrm{d}E$ integrated in three different regions versus incident energy E. (a) The curve shows $\mathrm{d}N_{11}/\mathrm{d}E$ in the region Ω_{III}. (b) The solid line is in the region Ω_{II} and the dotted line is in the region Ω_{I}.

counterpart. In the classical and WKB approximations, $\mathrm{d}n_{11}(x)/\mathrm{d}E$ or $\mathrm{d}N_{11}/\mathrm{d}E$ is always zero in the region Ω_{III} [31]. Comparing figure 6(a) with figure 6(b), we find that this quantum effect is very small, and is about 1% in the region Ω_{I} and 6% in the well. However, the global density of states $\mathrm{d}N_{21}/\mathrm{d}E$ does not oscillate. It is always positive—see figure 7—since the total DOS and the transmission probabilities are always positive. At resonant energies, the GPDOSs of $\mathrm{d}N_{21}/\mathrm{d}E$ reach their maxima, as shown by the dashed line in figure 7. In other regions, the peak is low.

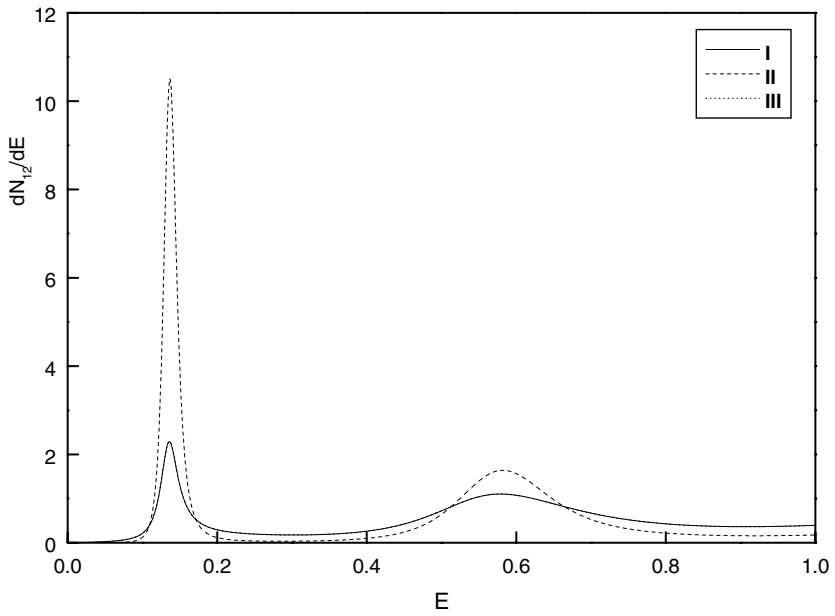

Figure 7. The global PDOS $\mathrm{d}N_{21}/\mathrm{d}E$ integrated in three regions. The solid line is in the region Ω_{I}. The dashed line is in the region Ω_{II}. The dotted line is in the region Ω_{III} and exactly equal to the solid line.

The physically measurable quantities are injectivity and emissivity. In the absence of magnetic field, the injectivity is equal to the emissivity [9]. Thus, we plot the injectivity for discussion, and assume the particles to be incident from probe 1 (see figure 2). Figure 8 shows the distributions of injectivities at different incident energies. It can be seen that the behaviours in the three regions are different. The typical characteristic is that for all incident energies the injectivities in the region Ω_{III} are constant. In our simplified model, the wavefunctions in the region Ω_{III} are plane waves and $\mathrm{d}n_{\alpha}(x)/\mathrm{d}E$ is equal to $|\psi_{\alpha}(x)|^2/hv_{\alpha}$ [16]. Here, $\psi_{\alpha}(x)$ is a wavefunction of a particle incident from probe α. It can be predicted from this expression that the injectivities will be constant in the region Ω_{III}. It is interesting to see in figure 8(c) that the full quantum quantity of the LPDOS, $\mathrm{d}n_{11}(x)/\mathrm{d}E$, can be compared to $\mathrm{d}n_{12}(x)/\mathrm{d}E$ in the region Ω_{III}. The amplitude of this quantity is of the same order as $\mathrm{d}n_{12}(x)/\mathrm{d}E$. However, in many important calculations this quantity is neglected [16]. As mentioned above, the WKB approximation and quasi-classical approximation give none of this value. From figure 8(c) we can see that $\mathrm{d}n_{12}(x)/\mathrm{d}E$ is positive but $\mathrm{d}n_{11}(x)/\mathrm{d}E$ can be positive or negative. The sum of $\mathrm{d}n_{12}(x)/\mathrm{d}E$ and $\mathrm{d}n_{11}(x)/\mathrm{d}E$ is constant. So, in the full quantum calculations we must involve the contributions of $\mathrm{d}n_{11}(x)/\mathrm{d}E$.

The total density of states in the well is plotted in figure 9. It is clear that at the resonant energy the total DOS reaches its largest value. The width of the peak becomes

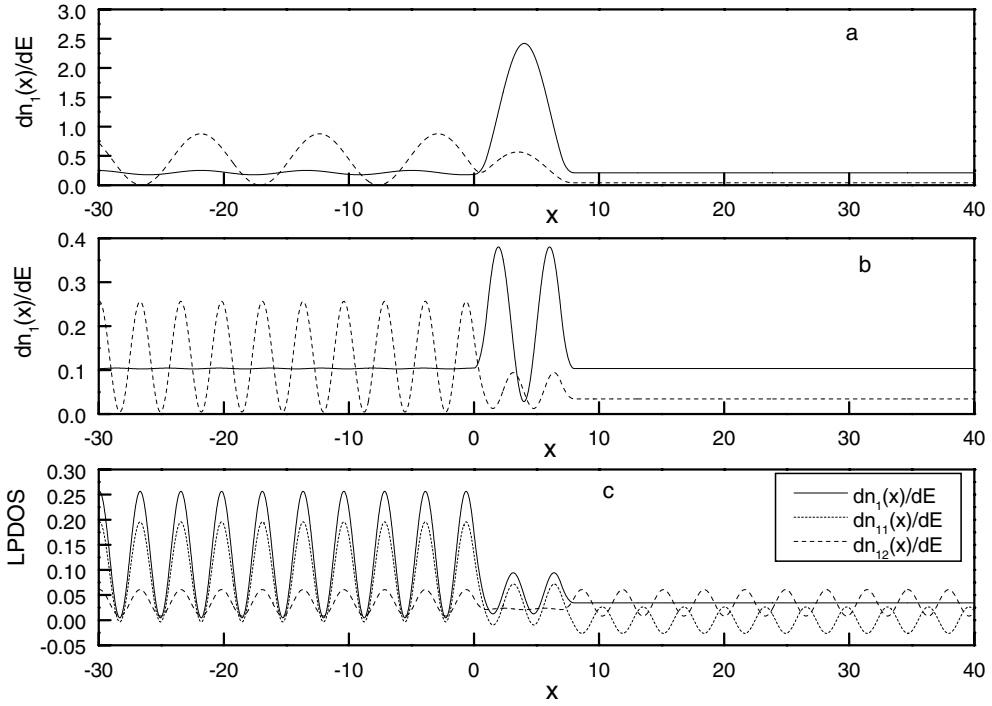

Figure 8. The distribution of the injectivity $\mathrm{d}n_1(x)/\mathrm{d}E$ in real space and a comparison with its components $\mathrm{d}n_{11}(x)/\mathrm{d}E$ and $\mathrm{d}n_{12}(x)/\mathrm{d}E$ versus the incident energies. (a) The solid line is $\mathrm{d}n_1(x)/\mathrm{d}E$ at E_2 and the dashed line is at E_1. (b) The solid line is at incident energy E_3 (resonant) and the dashed line is at E_4. (c) The solid line is the local injectivity $\mathrm{d}n_1(x)/\mathrm{d}E$, the dashed line is $\mathrm{d}n_{12}(x)/\mathrm{d}E$, and the dotted line is $\mathrm{d}n_{11}(x)/\mathrm{d}E$ at E_4.

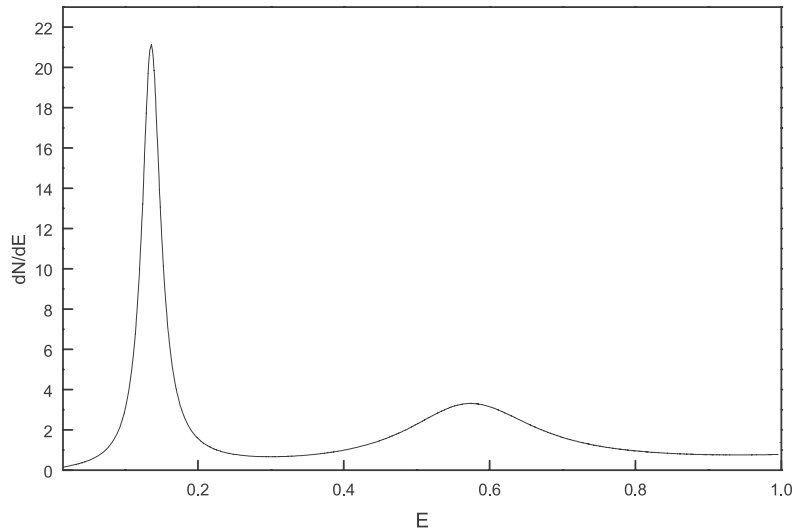

Figure 9. The total density of states $\mathrm{d}N(\Omega_{\mathrm{II}})/\mathrm{d}E$ in the well. (A comparison of the numerical and analytical method has been carried out. The DOS and the injectivity are exactly the same within the numerical precision.)

wider as the incident energy increases. This result is consistent with those obtained by other methods [32].

4. Conclusions

We have investigated the partitioned densities of states and their global characteristics. A brief derivation gives a clear physical picture of this kind of decomposition. Numerical results are derived to provide a better understanding of the meaning of this partitioning. We found not only that the total density of states is important, but also that the partitions of the DOS are needed in transport problems. Generally, in calculating the AC admittance, the PDOS and LPDOS cannot be neglected in the nonclassical regime. Our derivation indicates that the internal potential variations have a great influence on the partitioned DOS.

Acknowledgments

The author thanks Professor Y X Chen for encouragement to do this work, and the University of Hong Kong for providing computing facilities.

References

[1] Huang K 1987 *Statistical Mechanics* (New York: Wiley) p 225
Callaway J 1991 *Quantum Theory of the Solid State* (New York: Academic) p 400
[2] Abrikosov A A 1988 *Fundamentals of the Theory of Metals* (Amsterdam: North-Holland) p 218
[3] Esaki L 1974 *Rev. Mod. Phys.* **46** 237
[4] Dashen R, Ma S K and Bernstein H J 1969 *Phys. Rev.* **187** 345
[5] Datta D 1995 *Electronic Transport in Mesoscopic Conductors* (New York: Cambridge University Press) p 196
[6] Ferry D K and Goodnick S M 1997 *Transport In Nanostructures* (Cambridge: Cambridge University Press) p 23
[7] Imry Y 1997 *Introduction to Mesoscopic Physics* (New York: Oxford University Press) p 89
[8] Büttiker M 1992 *Phys. Rev.* B **46** 12 485
Khondker A N and Alam M A 1992 *Phys. Rev.* B **45** 8516 and references therein
[9] Büttiker M 1993 *J. Phys.: Condens. Matter* **5** 9361
[10] Büttiker M, Thomas H and Prêtre A 1994 *Z. Phys.* B **94** 133
[11] Ma Zhong-shui, Wang Jian and Guo Hong 1999 *Phys. Rev.* B **59** 7575
[12] Büttiker M, Prêtre A and Thomas H 1993 *Phys. Rev. Lett.* **70** 4114
[13] Prêtre A, Thomas H and Büttiker M 1996 *Phys. Rev.* B **54** 8130
[14] Gasparian V, Christen T and Büttiker M 1996 *Phys. Rev.* A **54** 4022
[15] Wang J and Guo H 1996 *Phys. Rev.* B **54** R11 090
[16] Büttiker M and Christen T 1996 *Quantum Transport in Semiconductor Submicron Structures* ed B Kramer (Dordrecht: Kluwer–Academic)
[17] Gramespacher T and Büttiker M 1998 *Phys. Rev. Lett.* **81** 2763
[18] Zhao Xuean, Wang Jian and Guo Hong 1999 *Phys. Rev.* B **63** 16 730
[19] Büttiker M 1995 *Japan. J. Appl. Phys.* **34** 4279
Christen T and Büttiker M 1996 *Phys. Rev.* B **53** 2064
[20] Wan C C, Mozos J-L, Wang J and Guo H 1997 *Phys. Rev.* B **55** R13 393
[21] Zheng Q, Wang J and Guo H 1997 *Phys. Rev.* B **56** 12 462
[22] Gasparian V, Ortuno M, Cuevas E and Ruiz J 1996 *Solid State Commun.* **97** 791
Büttiker M 1983 *Phys. Rev.* B **27** 6
[23] Hammouchi M, El Boudouti E H, Nougaoui A and Djafari-Rouhani B 1998 *J. Phys.: Condens. Matter* **10** 2039
[24] Leavens C R 1998 *Superlatt. Microstruct.* **23** 795 and references therein
[25] Economou E N 1979 *Green's Functions in Quantum Physics* (Heidelberg: Springer) p 7
[26] Iannaccone G 1995 *Phys. Rev.* B **51** 4727
[27] Mizuta H and Tanoue T 1995 *The Physics and Applications of Resonant Tunnelling Diodes* (Cambridge: Cambridge University Press)

[28] Feynman R P and Hibbs A R 1965 *Quantum Mechanics and Path Integrals* (New York: McGraw-Hill) p 170
[29] Khondker A N and Haque A 1997 *Phys. Rev.* B **55** 15 798
[30] Datta S 1990 *J. Phys.: Condens. Matter* **2** 8023
Datta S 1992 *Phys. Rev.* B **45** 1347
Datta S 1992 *Phys. Rev.* B **45** 13 761
Mclennan M J, Lee Y and Datta S 1991 *Phys. Rev.* B **43** 13 846
[31] Christen T and Büttiker M 1996 *Phys. Rev. Lett.* **77** 143
[32] Trzeciakowski W, Sahu S and George T F 1989 *Phys. Rev.* B **40** 6058
Büttiker M 1988 *IBM J. Res. Dev.* **32** 63